Kinetics of the Epitaxy and the Over-growth of Polyoxymethylene from Molten State on Needle-like Single-crystals

Masatoshi Iguchi and Yasushi Watanabe

Kinetic studies have been made on the over-crystallisation of polyoxymethylene on needle-like crystals, which takes place cylindrically around the needles by forming a pile of lamellar crystallites, using the ordinary spherulitic crystallisation as reference. The growth kinetics were investigated, by means of microscopy and differential scanning calorimetry (DSC), and the resultant structure was examined by small-angle X-ray scattering and melting temperature measurements. The discontinuity found for their theoretical plot was assumed to be attributable to the difference in the type of crystallisation. The lamellar surface free energies obtained for the over-growth were smaller than those for the spherulitic growth, i.e., $\sigma_e = 42.1$ and $\sigma_s = 2.94$ erg/cm^2 against $\sigma_e = 53.4$ and $\sigma_s = 4.97$ erg/cm^2. The epitaxy effect was elucidated from the analysis of DSC curves during cooling and the combined free-energy, $\sigma_e\sigma_s = 89.4$ erg^2/cm^4, was estimated for the initial deposit on the needle surface.

1. INTRODUCTION

The kinetics of crystallisation has been a major subject ever since the dawn of polymer physics, when the mathematical theory to correlate the volume transformation to geometrical models, later called Avrami model, was devised. As many synthetic polymers appeared, rigorous investigations were made for the processes of crystallisation as well as the resultant morphology. After the discovery of the lamellar crystallisation habit and the chain folding, theories to describe the mechanism and the resultant structures were launched and applied to interpret the experimental results. Comprehensive reviews for these fields have been given in many places, e.g., in books by Geil [1] and Mandelkern,[2] compiling important theoretical developments by Turnbull, Lauritzen, Hoffman, Price and many other contributors. An excellent instructive monograph to the philosophical backgrounds was authored by Professor Manfred Gordon,[3] whose sixtieth birthday we jointly celebrate in these commemorative issues.

For polyoxymethylene, a number of papers have been published since the polymer became available as a stable material and the crystallisation made reproducible. Among them, the kinetics of spherulite growth as well as the resultant structure were studied theoretically by Baer and Carter.[4,5] The over-crystallisation on needle-like polyoxymethylene crystals,[6,7] forming a sort of cylindrite comprising a pile of lamellae around the slender core, viz. from molten polymers,[7] is clearly of interest in comparison with the normal, spherulitic crystallisation. In this paper, the kinetics of this crystallisation have been studied for polyoxymethylene diacetate. The growth rate was investigated by means of microscopy and the analysis of DSC (differential scanning calorimetry) isotherms at various temperatures and the resultant structure were examined by small-angle X-ray scattering and melting temperature measurements. This has cast light on the lamellar surface energies. To clarify the epitaxy or the nucleation effect, in particular, DSC curves during constant rate cooling were analysed on the basis of theoretical expressions derived for this purpose. Numerical calculations and curve fittings have been made on a digital computer to minimize the effects of human prejudice.

Research Institute for Polymers and Textiles, 4–1, Sawatari, Kanagawa-ku, Yokohama 221, Japan.

2. EXPERIMENTAL

2.1 Samples

Polyoxymethylene diacetate used was a commercial polymer, Delrin 500X, $\bar{M}_v = 1.57\times10^5$, from E. I. du Pont de Nemours Co. The procedures for preparing needle-like crystals [8–10] and embedding them in the matrix polymer [7] were as described in those references. The average needle content was 1%.

2.2 Differential Scanning Calorimetry (DSC) and Other Measurements

DSC-2, of Perkin-Elmer Co., was used. For *in situ* crystallisation, the specimen, either the neat polymer or the needle/polymer mixture, was placed in the cell and heated at 455 K for 2 min to remelt the matrix alone, before the temperature was lowered for crystallisation. For isothermal crystallisation, the initial cooling rate was 40 K/min. For the temperature calibration and the measurement of melting temperature similar procedures and precautions were employed as on previous occasions.[11] The method of X-ray measurement was reported before.[12] The computer used was a HITAC 8450 of this institute, accepting ALGOL/FORTRAN programs.

3. RESULTS AND DISCUSSION

3.1 Isothermal Growth Rate

The increase in radius during the spherulitic and the cylindritic growth was measured, at various temperatures, from each series of micrographs such as is shown in Figure

Table 1. Radial growth rate, g of spherulite and cylindrite at various temperatures, T_c

Method	Tc (K)	g (μm/min)	ln g	ln g + (1/3) lnC
Spherulite Growth				
Microscopy	433.0	24.5	3.20	
	432.0	10.0	2.30	
	434.0	3.75	1.32	
	435.5	1.64	0.49	
DSC[a]	425.0	284	5.65	0.65
	427.0	122	4.80	−0.20
	429.0	45.2	3.81	−1.19
	431.0	15.3	2.73	−2.28
	433.0	5.42	1.69	−3.31
	435.0	1.91	0.65	−4.35
Cylindrite Growth				
Method	Tc (K)	g (μm/min)	1n g	1n g + (1/2) 1n C
Microscopy	431.5	6.56	1.88	
	433.5	2.88	1.06	
	435.5	1.23	0.206	
	436.5	0.820	−0.196	
	438.0	0.449	−0.801	
	439.5	0.237	−1.44	
	441.0	0.106	−2.25	
	443.0	0.031	−4.39	
DSC[b]	433.0	3.39	1.22	−0.48
	435.0	1.21	0.19	−1.51
	437.0	0.711	−0.34	−2.04
	439.0	0.261	−1.34	−3.04
	441.0	0.105	−2.25	−3.95

a (1/3) ln C = −5.00, *b* (1/2) ln C = −1.70.

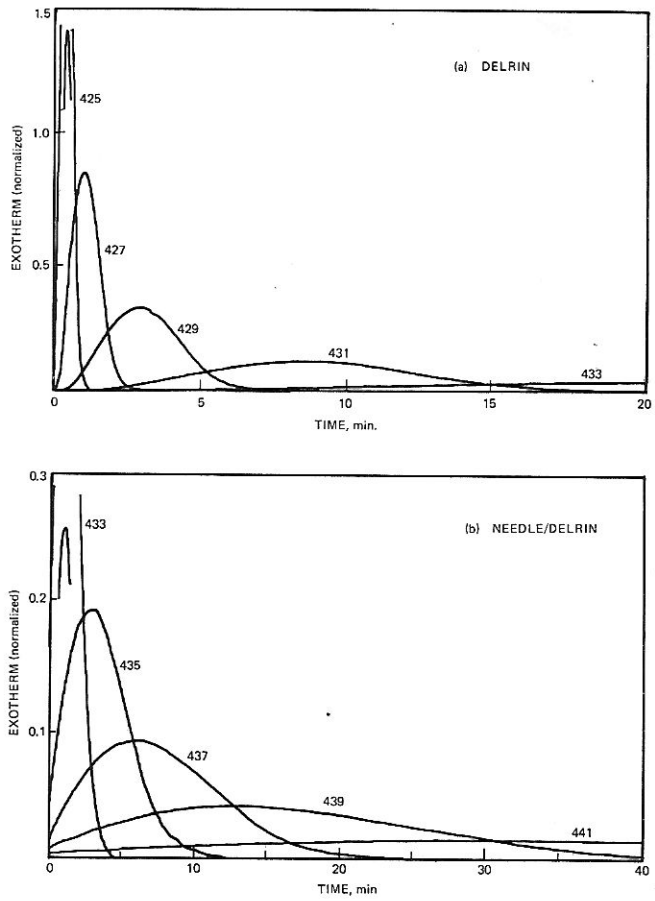

Fig.1 DSC crystallisation isotherms of Delrin at various temperatures, (a) without needle-like crystals and (b) with 1% needles embedded. The curves have been normalised to the unit area. The figures denote crystallisation temperatures (K).

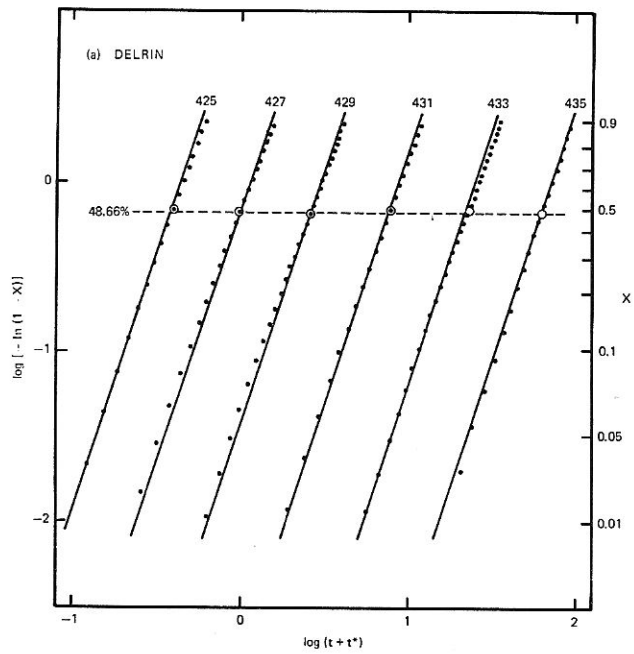

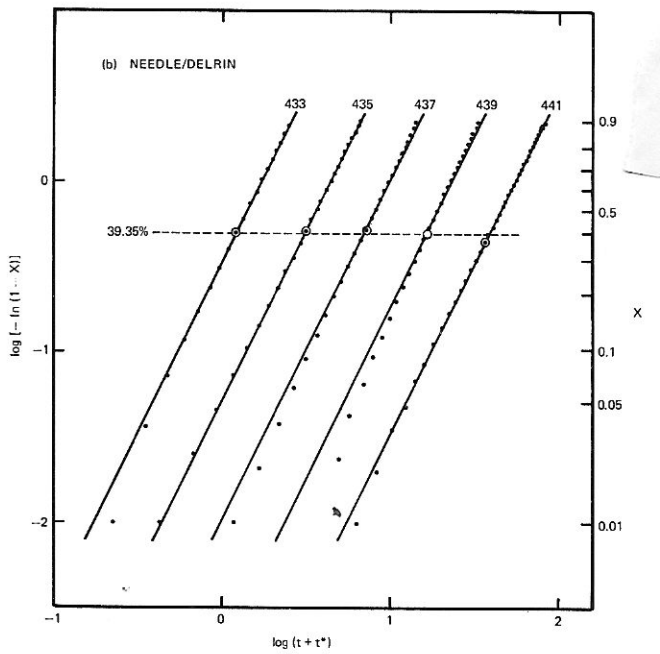

Fig.2 Double-logarithm plots for the crystallisation of Delrin, (a) without needle-like crystals forming spherulites and (b) with needles embedded forming cylindrites. The lines have been drawn with slopes 3 and 2, in (a) and (b), respectively.

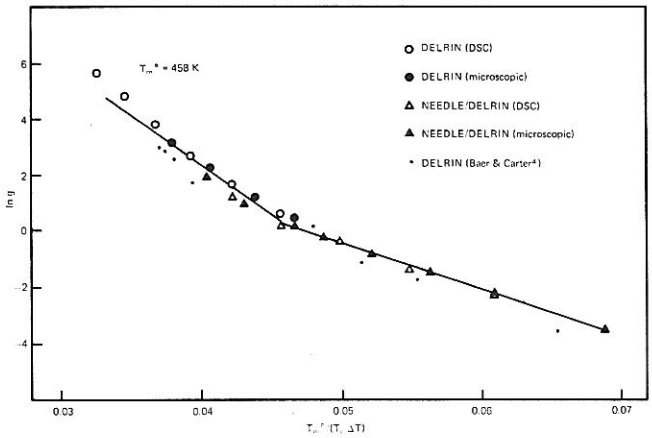

Fig.3 Plots to correlate the growth rate, g and the crystallisation temperature, T_c, according to equation (4). T_m° = 458 K was assumed.

1 of reference 7. For both cases, the sizes of growing bodies observed were almost homogeneous and good linearity was established against time for every run. The growth rate, calculated as usual from the slope, is listed in the third column of Table 1. For the two types of growths, measurements were not made in a common temperature region. Without needles, spherulite growth was virtually impossible above 436 K, because of the difficulty in nucleation from the homogeneous melt. (It would not be impossible, if the melting were not complete to erase the previous 'memory'.) On the other hand, to follow the overgrowth below 431 K was difficult, since the cylindrites grow to large size before the isothermal condition can be reached. Concerning spherulite growth, similar measurements for this polymer were originally reported by Baer and Carter;[4] the agreement is not unsatisfactory, as shown in Figure 3.

The DSC isotherms obtained with the neat polymer and the polymer/needle mixture, at various temperatures, are shown in Figure 1. It is remarked that the curves from the mixture are non zero at time zero, implying the absence of an induction time, and seem to be broader, reflecting the change of growth habit from three to two dimensional. As justified by Kamide *et al*,[13] the height of DSC isotherms may be assumed, to a first approximation, to be proportional to the rate of mass transformation, dX/dt, i.e., the change in the degree of crystallinity, X, with time, t. In general, a crystallisation in bulk system should involve two processes, nucleation and growth. However, the microscopic evidence [7] and the appearance of DSC curves have indicated nucleation is concluded after a very short time. Then, X is related to the linear growth rate, g, by the Avrami-type expression,

$$-\ln(1-X) = C\,[g(t+t^*)]^n \qquad (1)$$

where

$$t^* = R_0/g \qquad (2)$$

Here, the time-correction parameter, t^* is for the radius of needles, R_0 (*ca.* 1.0 μm), which is not negligible; for the analysis of experimental data, it may also cover the error in fixing the initial time. 'n' is an integer constant for the growth dimension and C, a constant involving the shape factor and the nucleation density.

For the curves of Figure 2, n as well as t^*, was calculated by least-squares fitting to the equation derived by Banks *et al.*[14]

$$-(1-X)\ln(1-X)/(dX/dt) = (1/n)(t+t^*) \qquad (3)$$

As expected from the habits, the values of n fell in the vicinity of 2 and 3 (i.e, 2.08 ± 0.10 and 2.81 ± 0.11), for the families of curves with and without needles, respectively. Figure 2 demonstrates the fitting using the usual double-logarithm plot; the encircled points mark the maxima of dX/dt vs. t curves (Figure 1), where X should be uniquely 39.35 and 48.66% for n = 2 and 3, respectively.[15]

The quantities, $\ln(C^{1/n}\,g)$, obtained are listed in the last column of Table 1. For the over-crystallisation, C is predicted to be a constant for the epitaxy mechanism (on a given needle surface area). When $\ln(C^{1/2}\,g)$ was plotted, together with $\ln g$ (Column 4), against T, the two kinds of plots were superposed with a single shift factor, $\ln C^{1/2}$.

For the free crystallisation also, similar superposition was obtained, at least above 430 K, suggesting that the nucleation might be aided by some clusters which existed in the 'neat' polymer. The values of $\ln g$ (and g) thus deduced are listed in the second and the third column of Table 1, respectively.

3.2 Free Energies for Growth

Generally, the source mechanism of a linear crystal growth is considered to be a secondary nucleation. For the layer-like deposit of molecules on existing surfaces, with chain folding,[1,2]

$$\ln g = \ln K - (4\,\sigma_e\sigma_s\,b/k\Delta H_u)\,(T_m^\circ/T_c\Delta T) \qquad (4)$$

where T_m° is the equilibrium melting temperature of the polymer, ΔT (= $T_m^\circ - T_c$), the under-cooling, ΔH_u, the heat of transformation, b, the monomolecular layer thickness, and σ_e and σ_s are the end and the side surface energies, respectively. The first term K, relating to molecular transport, is regarded to be constant.

From the morphological evidence, both spherulitic and cylindritic growths are considered to obey this mechanism so that the growth rates, obtained above, are directly applicable to equation (4). (Correction, if necessary for molecular tilt in lamellae, may be covered by the constant, K.) T_m° of polyoxymethylene, as determined by various reported methods was distributed [11,16] over a wide range from 453 to 483 K; the value measured carefully with the needle-like crystals was 456–458 K.[11] The plot in Figure 3 was made adopting T_m° = 458 K. The result showed that to cover the whole range of plots by a single slope was difficult. When T_m° was floated and fitted to equation (4), the magnitude of misfit from a single slope decreased gradually with increasing T_m° and tended to level off at above 480 K. (The temperature was similar to that from extraporation of the spherulitic growth data[5].) The deviation was still systematic, however. Bringing T_m° to infinity in equation (4) is equivalent to assuming another theoretical formula based on a kink-deposit model, in which T_m° should have nothing to do with the linearity any longer; this plot was not successful either, resulting in a larger error. Various approximations used in deriving the equations were checked to find no improvement.

In consequence, the coefficient in the last term of equation (4), *viz.* $\sigma_e\sigma_s$, was considered to vary with $T_m/(T_c\Delta T)$. Turning back to Figure 3, the plots appear to comprise two linear parts with different slopes in the high and low temperature regions, centred at around

Table 2. Peak nucleation under-cooling, u^* (and the corresponding temperature, T^*) during cooling at constant rates, r, deduced from DSC curves using equations (11) and (12).

	Free nucleation				*Epitaxy*			
r (K/min)	T_0 [a]	T^*	u^* [b]	$Cx10^6$	T_0 [a]	T^*	u^* [b]	$Cx10^2$
0.313	434.8	436.6	21.4	0.61	443.4	442.8	15.2	5.28
0.625	433.8	434.6	23.4	0.99	442.8	442.0	16.0	4.27
1.25	432.4	433.2	24.8	1.66	441.6	440.2	17.8	3.41
2.5	431.2	431.8	26.2	3.20	440.2	438.6	19.4	3.17
5	429.6	430.3	27.8	4.99	438.6	436.4	21.6	4.36
10	428.6	428.8	29.2	4.72	436.6	434.2	23.8	4.59
20	426.0	426.6	31.4	2.97	434.4	431.8	26.2	5.24

a Initial temperature where curves depart from base lines.
b $T_m^o = 458$ K.

$T_m/(T_c\Delta T) = 4.6x10^{-2}$, or $T_c = 435$ K, discounting the scatter in the intermediate region. This can be explained simply if a speculation is permitted that the two slopes represent cylindritic and spherulitic growth, respectively. The value of the combined free energy, $\sigma_e\sigma_s$ calculated were 132 and 286 erg^2/cm^4, respectively (with ΔH_u = $2.116x10^9$ erg/cm^3 ref.11 and $b = 8.92x10^{-8}$ cm).

The melting temperature, T_m, and the reciprocal of the X-ray long spacing, L, measured for isothermally crystallised specimens, are plotted in Figure 4, according to the common equation.[1,2]

$$T_m = T_m^o\ [1 - (2\sigma_e/\Delta H_u)/L] \qquad (5)$$

The expected linearity appeared to be broken up at around $1/L = 4.2x10^{-3}$ A^{-1} or $T_c = 435$ K, corresponding to the previous plot (Figure 3). Then, two slopes shown were drawn towards $T_m^o = 458$ K. The end free energies, $\sigma_e = 42.1$ and 53.4 erg/cm^2 were calculated for the upper and the lower temperature regions, respectively, and applied to the values of $\sigma_e\sigma_s$, obtained above, to estimate σ_s = 2.94 and 4.97 erg/cm^2.

From these results, it is inferred that the regularity of the lamellae formed by the over-growth mechanism is higher, bearing smaller surface free energies, compared with that by the ordinary spherulite growth. However, it is difficult to make these arguments more quantitative. Whether or not our assumption of two regions is adequate, the method using equations (4) and (5), depends sensitively on the choice of parameters, viz T_m^o and ΔH. In fact, the values of σ_e and σ_s for the spherulite growth of this polymer, reported in literatures,[4,5,17–19] are distributed over broad ranges, 37–153 and 3.3–14.3 erg/cm^2, respectively.

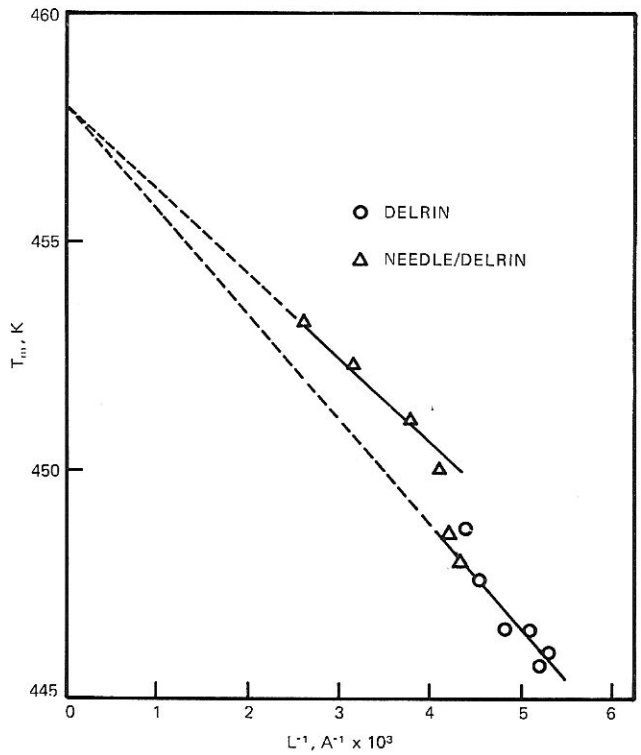

Fig.4 Relation between the melting temperature, T_m, and the reciprocal of X-ray long-spacing, L, for isothermally crystallised specimens. The slopes were drawn pointing at $T_m^o = 458$ K.

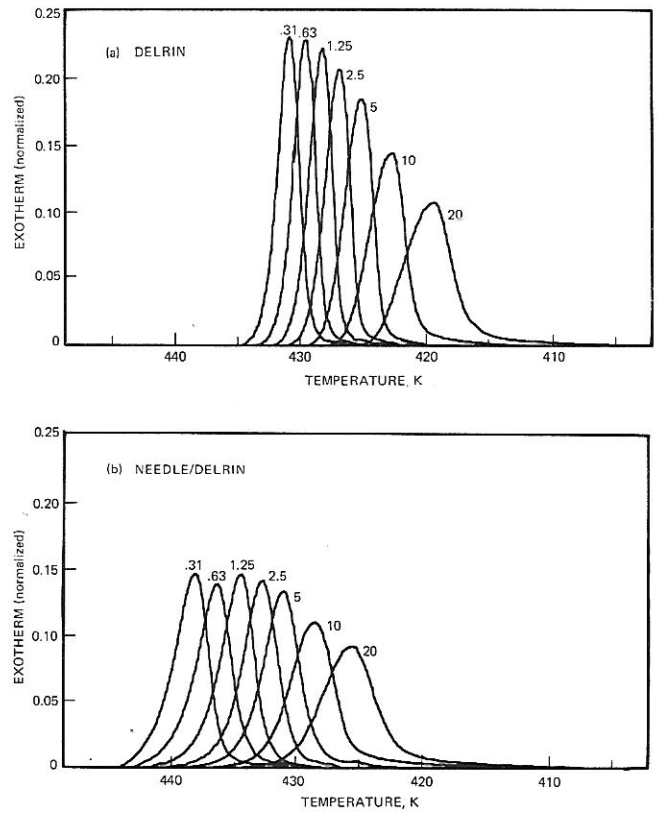

Fig.5 DSC crystallisation curves during constant-rate cooling, of Delrin, at various rates indicated (K/min.), (a) without needle-like crystals and (b) with 1% needles embedded. The curves have been normalised to the unit area.

3.3 Transformation during Cooling

In preliminary experiments,[7] DSC curves during cooling were more informative for nucleation or epitaxy effect. The detailed runs at various cooling rates are shown in Figure 5, for the neat polymer and the polymer/needle mixture. The change with the cooling rate was quite systematic and, in the presence of needles, the exotherm appeared much earlier.

In order to describe such DSC curves, let us assume two functions, $\phi(u_i)$, the frequency (normalised) of nucleation or surface activation at under-cooling, u_i and $v(u,u_i)$, the volume at u of each body, supposedly growing free without overlapping or impingement. Allowing for impingement, the overall crystallinity, X, is given by,

$$-\ln(1-X) = \int_0^u C\,\phi(u_i)\,v\,(u, u_i)\,du_i \qquad (6)$$

where C is the nucleation density. For spherical or cylindrical growth, $v\,(u, u_i)$ can be a simple function of radius, R. Next, the growth rate, g, obtained at fixed temperatures, is assumed to be continuous function of T or u. Since $du/dt = r$ during the cooling at constant rate, r,

$$dR/du = (1/r)\,g(u) \qquad (7)$$

Then the net increase of the radius between u_i and u is,

$$R\,(u, u_i) = \int_{u_i}^{u} (1/r)\,g\,(u')\,du' \equiv (1/r)\,G(u, u_i) \qquad (8)$$

Using this expression, equation (6) is specialised as follows. For spherical growth,

$$-\ln\,(1-X) = \int_0^u C\,\phi\,(u_i)\,[(1/r)\,G\,(u, u_i)]^3\,du_i \qquad (9)$$

and for cylindrical growth from nuclei of original radius R_0,

$$-\ln\,(1-X) = \int_0^u C\,\phi\,(u_i)\,\{\,[(1/r)\,G\,(u, u_i) + R_0]^2 - R_0^2\,\}\,du_i - CR_0^2 \qquad (10)$$

Here, C involves the shape factor for each growth type. If the nucleation takes place rapidly in the initial stage at under-cooling u^* and $\phi\,(u)$ is approximately a delta-function, equations (9) and (10) reduce to equations (11) and (12), respectively.

$$-(1-X) = C\,[(1/r)\,G\,(u, u^*)]^3 \qquad (11)$$

and

$$-(1-X) = C\,[(1/r)\,G\,(u, u^*) + R_0]^2 \qquad (12)$$

The data were not accurate enough to allow $\phi\,(u)$ to be obtained for the curves of Figure 5 by numerical solution of equations (9) and (10). The results suggested, however, that $\phi\,(u)$ was very narrow. Consequently equations (11) and (12) were employed and the value of u^* was allowed to float over a wide range, at 0.2 K intervals, searching for the optimum value by least-squares fitting. The results listed in Table 2 were obtained, in the fitting range, $0.1 < X < 0.35$, by assuming $R_0 = 1.0\ \mu m$ and taking $g(u)$ from the two slopes of Figure 3.

In Table 2, u^* was also converted to T^* (by $T_m^\circ = 458$ K) and compared with T_0, the temperature at which the curves in Figure 5 departed from the baseline, or the exotherm became appreciable. For spherulite formation, T^* were always found shortly before T_0, in agreement with the view that the process was nucleation-controlled. 'u^*' for the over-crystallisation appeared shortly after T_0. The values of C, obtained simultaneously with u^*, are also listed in Table 2. The fitting was not necessarily appropriate for the determination of this constant, but the result is at least qualitatively suggestive. For the over-crystallisation, C, corresponding to the surface area for the epitaxy, or the amount of embedded needles, may be regarded as constant. For the spherulite formation, the values are scattered but seem to be the same order between runs, except those of low cooling rates.

3.4 Dependence of the Nucleation Temperature on the Cooling Rate

The distribution of nucleation frequency in a system is related to its volume free-energy to form a critical nucleus, W^*. If X, the transformed volume fraction is small at the stage of nucleation,[20]

$$r\,\phi\,(u) = K \exp\,[-W^*/k\,(T_m^\circ - u)]\;[1 - \psi\,(u)] \qquad (13)$$

where

$$\psi\,(u) = \int_0^u \phi\,(u')\,du' \qquad (14)$$

W^* depends on the type of nucleus assumed. For the surface nucleation depositing molecules in a rectangular shape on an existing crystal surface,

$$W^* = 4\sigma_e\sigma_s b\,T_m^\circ/\Delta H_u u \qquad (15)$$

and for the formation of a cylindrical bundle of molecules, free from surface effects,

$$W^* = 8\pi\sigma_e\sigma_s^2\,T_m^{\circ 2}/\Delta H_u^2\,u^2 \qquad (16)$$

The former model represents the growth process written by equation (4).

To make use of these equations for the analysis of experiments, a derivation was made by Burns and Turnbull [20] involving some approximations. Another derivation is now possible. For the case of the surface nucleation, equations (13) and (15) give;

$$r\,\phi(u) = K \exp[-a_1\, T_m{}^\circ/(T_m{}^\circ - u)\,u]\;[1 - \psi(u)] \quad (17)$$

where

$$a_1 = 4\,\sigma_e\sigma_s b/k\Delta H_u \quad (18)$$

Differentiating equation (17) by u and setting $\phi'(u) = 0$, to find the maximum of $\phi(u)$, followed by arranging,

$$-\ln\,[r\,(T_m{}^\circ - 2u)\,T_m{}^\circ/(T_m{}^\circ - u)^2u^2]$$

$$= a_1\,T_m{}^\circ/(T_m{}^\circ - u)\,u - \ln(K/a_1) \quad (19)$$

Thus, the parameter a_1 (as well as K) can be evaluated from the peak under-cooling of $\phi(u)$ at various cooling rates. For the free nucleation the same procedure gives, from equations (13) and (16);

$$-\ln\,[r\,(2T_m{}^\circ - 3u)\,T_m{}^{\circ 2}/T_m{}^\circ - u)^2u^3]$$

$$= a_2 T_m{}^{\circ 2}/(T_m{}^\circ - u)u^2 - \ln(K/a_2) \quad (20)$$

where

$$a_2 = 8\pi\sigma_e\sigma_s{}^2/k\Delta H_u{}^2 \quad (21)$$

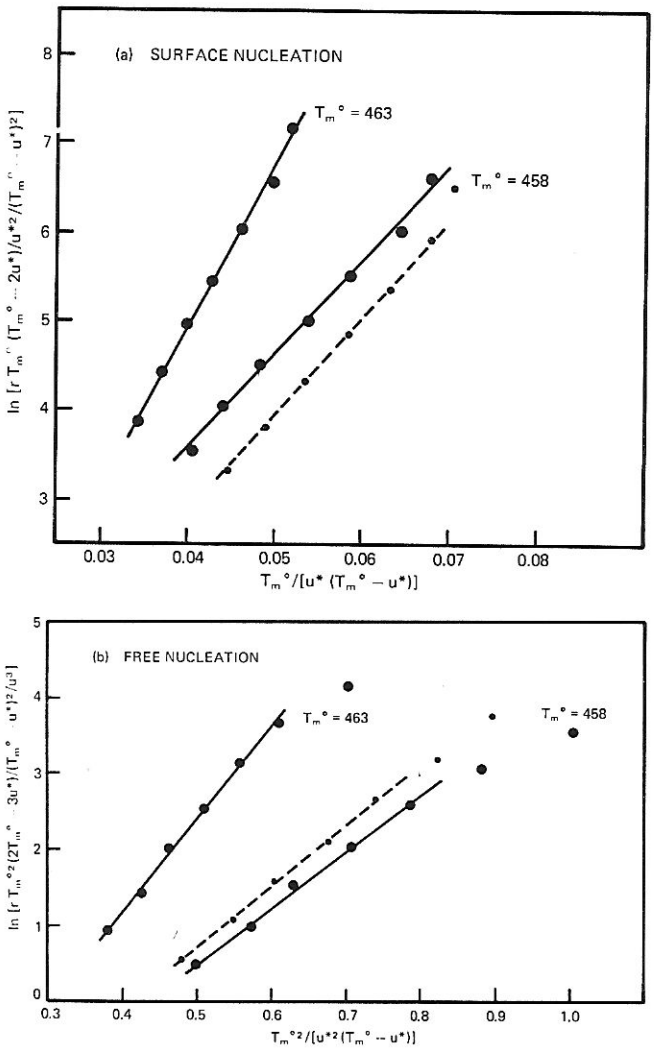

Fig.6 Plots to correlate the peak nucleation under-cooling, u^* and the cooling rate, r; (a) for the epitaxy upon needle-like crystals, according to equation (19), (b) for the free nucleation, according to equation (20). Small points/broken lines show the relation with u_0, used in place of u^*. Plots with $T_m{}^\circ$ = 463 K are also shown just for reference.

These equations could be easily approximated by the previous simpler expressions,[20] in which u was characterised at $\phi(u) = 0.5$, instead of $\phi'(u) = 0$, however.

The values of u^* obtained above (Table 2) were assumed to satisfy $\phi'(u) = 0$. Figure 6 (a) shows the plot for the needle/polymer mixture based on equation (19), i.e., the surface-nucleation model. A reasonable linearity was obtained and the combined free-energy, $\sigma_e\sigma_s$ = 89.4 erg^2/cm^4 was calculated from the slope, while that for the growth process was 132 erg^2/cm^4 (Section 3.2). (A similar result was obtainable by plotting u_0 (= $T_m{}^\circ - T_0$).) The slope itself depends, once again, upon the choice of $T_m{}^\circ$, but this comparison suggests that the surface energies for the epitaxy or the initial deposit of molecules are smaller than that for the subsequent deposit process. This can explain the fact that the epitaxy was almost simultaneous on all needle surfaces and then the growth followed smoothly. A similar plot of u^* for the nucleation in the neat polymer, based on equation (19), is shown in Figure 7 (*b*), the slope giving $\sigma_e\sigma_s{}^2$ = 192 erg^3/cm^6. Further development of arguments of this kind would not be very meaningful, however, because of the intuitive nature of the bundle-like nucleus model adopted.

4. CONCLUSION

The understanding of over-crystallisation on needle-like polyoxymethylene single-crystals, previously studied by the visual and other qualitative techniques, has been rendered more quantitative, with reference to the normal, spherulitic crystallisation. The discontinuity found in theoretical plots of kinetic results was assumed to be attributable to the alteration between the two types of nucleation/growth; the lamellar surface energies obtained were smaller for the over-growth than those for the spherulite growth, i.e., σ_e = 42.1 and σ_s = 2.94 erg/cm^2 and σ_e = 53.4 and σ_s = 4.97 erg/cm^2, respectively. The over-growth process, giving a cylindrical morphology, was well described by the two-dimensional Avrami model. The epitaxy effect was made clear by analysis of DSC curves during constant-rate coolings; the surface free energies for the initial deposit of molecules was $\sigma_e\sigma_s$ = 89.4 erg^2/cm^4. The method of plotting the peak under-cooling of nucleation on the relations derived may be more generally applicable.

ACKNOWLEDGEMENTS

We thank Dr. J. W. Kennedy, of Essex University, for useful advice and correction of English. Thanks are also due to Miss T. Suzuki, of R.I.P.T., for technical assitance.

NOMENCLATURE

b:	monomolecular layer thickness, 8.92x10^{-8} cm.
C:	nucleation or surface-activation density, on occasion, multiplied by the shape factor for sphere or cylinder.
g:	radial growth rate of spherulite or cylindrite.
$g(u)$:	g as a function of under-cooling, u.
ΔH_u:	heat of fusion, 2.11$_6$x10^9 erg/cm^3.
K:	a kinetic factor for molecular and transport properties.
L:	lamellar thickness, represented by small-angle X-ray long-spacing.

n:	Avrami Constant.
R_0:	radius of needle-like crystals.
$R(u, u_i)$:	radius increase between under-coolings, u_i and u.
r:	cooling rate.
T_m^o:	equilibrium melting temperature, 458 K.
T_m:	observed melting temperature.
T_c:	crystallisation temperature (isothermal).
ΔT:	under-cooling.
t:	time.
t^*:	time-correction parameter standing for R_0/g.
u:	under-cooling ($\equiv\Delta T$).
u^*:	peak nucleation under-cooling.
$v(u,u_i)$:	volume of an unimpinged growing body at u (nucleated at u_i).
W^*:	volume-free energy to form a critical nucleus.
X:	transformed volume fraction or the degree of crystallinity.
$\phi(u)$:	frequency of nucleation or surface activation at u (normalised).
σ_e:	end-surface free energy of lamella.
σ_s:	side-surface free energy of lamella
$\psi(u)$:	fraction of nuclei or surface activated by u..

References

1 Geil, P. H., *Polymer Single-crystals,* Interscience Publishers, New York, London, Sydney 1963.
2 Mandelkern, L., *Crystallization of Polymers,* McGraw-Hill, Inc. New York, 1964.
3 Gordon, M., *High Polymers, Structures and Properties,* 2nd Ed., Iliffe Book Ltd., London, 1962.
4 Baer, E.; Carter, D. R. *J. Appl. Phys.* 1964, **35**, 1895.
5 Carter, D. R.; Baer, E. *ibid.* 1966, **37**, 4060.
6 Iguchi, M.; Murase, I. *J. Polym. Sci. A2* 1975, **13**, 1461.
7 Iguchi, M.; Watanabe, Y. *Polymer* 1977, **18**, 265 .
8 Iguchi, M. *Bri. Polym. J.* 1973, **5**, 195.
9 Iguchi, M.; Murase, I. *J. Cryst. Growth* 1974, **24/25**, 596
10 Iguchi, M.; Murase, I. *Makromolek. Chem.* 1975, **176**, 2113.
11 Iguchi, M. *ibid.* 1976, **177**, 549.
12 Iguchi, M.; Murase, I.; Watanabe, K. *Br. Polym. J.* 1974, **6**, 61.
13 Kamide, K.; Fujii, K. *Kobunshi Kagaku* 1968, **25**, 155.
14 Banks, W.; Gordon, M.; Roe, R-J.; Sharples, A., *Polymer* 1963, **4**, 61.
15 Godovskii, Yu. K.; Slonimskiĭ, G. L. *Vysokomolek. Soedin.* 1966, **8**, 403.
16 Jaffe, M.; Wunderlich, B. *Kolloid-Z. Z. Polymere* 1967, **216/217**, 203.
17 Ergoz, E.; Mandelkern, L. *J. Polym. Sci. B* 1973, **11**, 73.
18 Korenaga, T.; Hamada, F.; Nakajima, A. *Polymer J., Japan,* 1972, **3**, 21.
19 Hirai, N.; Tokumori, T.; Katayama, T.; Fujita, S.; Yamashite, Y. Rep. Res. Lab. Surface Sci. Okayama Univ. 1963, **2**, 91 (cited in Ref. 5).
20 Burns, J. R.; Turnbull, D. *J. Appl. Phys.* 1966, **37**, 4021.